MOLECULAR AND CELLULAR BIOLOGY, Feb. 1990, p. 501–509
0270-7306/90/020501-09$02.00/0

Vol. 10, No. 2

Molecular Analysis of Two Mouse Dilute Locus Deletion Mutations: Spontaneous Dilute Lethal^{20J} and Radiation-Induced Dilute Prenatal Lethal Aa2 Alleles

MARJORIE C. STROBEL, PETER K. SEPERACK,† NEAL G. COPELAND, AND NANCY A. JENKINS*

Mammalian Genetics Laboratory, BRI-Basic Research Program, National Cancer Institute-Frederick Cancer Research Facility, P.O. Box B, Frederick, Maryland 21701

Received 1 August 1989/Accepted 12 October 1989

The dilute (*d*) coat color locus of mouse chromosome 9 has been identified by more than 200 spontaneous and mutagen-induced recessive mutations. With the advent of molecular probes for this locus, the molecular lesion associated with different dilute alleles can be recognized and precisely defined. In this study, two dilute mutations, dilute-lethal^{20J} (d^{l20J}) and dilute prenatal lethal Aa2, have been examined. Using a dilute locus genomic probe in Southern blot analysis, we detected unique restriction fragments in d^{l20J} and Aa2 DNA. Subsequent analysis of these fragments showed that they represented deletion breakpoint fusion fragments. DNA sequence analysis of each mutation-associated deletion breakpoint fusion fragment suggests that both genomic deletions were generated by nonhomologous recombination events. The spontaneous d^{l20J} mutation is caused by an interstitial deletion that removes a single coding exon of the dilute gene. The correlation between this discrete deletion and the expression of all dilute-associated phenotypes in d^{l20J} homozygotes defines the d^{l20J} mutation as a functional null allele of the dilute gene. The radiation-induced Aa2 allele is a multilocus deletion that, by complementation analysis, affects both the dilute locus and the proximal prenatal lethal-3 (*pl-3*) functional unit. Molecular analysis of the Aa2 deletion breakpoint fusion fragment has provided access to a previously undefined gene proximal to *d*. Initial characterization of this new gene suggests that it may represent the genetically defined *pl-3* functional unit.

Classic genetic analysis of variant mouse phenotypes has defined numerous genetic loci and, in some cases, numerous alleles at a given locus. However, the physical basis for these mutations and an understanding of the impact of mutagenic events on gene expression have been impeded by difficulties in gaining molecular access to the mutated genes. The murine dilute (*d*) locus is among those rare loci for which extensive analysis at both the genetic and molecular levels is possible. A vast collection of spontaneous, chemical-induced, and radiation-induced dilute locus mutations have been generated. With the ever-increasing number of genomic and cDNA probes for the dilute locus, the physical detection and precise analysis of DNA alterations and rearrangements associated with individual *d* alleles can now be accomplished. As illustrated in this study, this combined molecular and genetic analysis is elucidating the gene product(s) and genomic organization not only of the *d* locus but also of other loci in the *d* region of mouse chromosome 9.

More than 200 spontaneous and induced dilute mutations have been identified (25). As typified by the original *d* coat color mutation of the mouse fancy, mice homozygous for this recessive mutation exhibit a washed-out ("diluted") coat color (34). Pigment production is normal in these mice (29); the coat color phenotype is associated with an abnormal, adendritic morphology of the neural crest-derived melanocytes (20).

The original dilute mutation is unique in exhibiting only the coat color phenotype. In contrast, most dilute alleles, when homozygous, manifest additional phenotypes. Animals of the spontaneous dilute-lethal (d^{l}) or mutagen-induced dilute-opisthotonic (d^{op}) class exhibit the neurological disorder of opisthotonus, a convulsive arching of the animal's head and neck (30, 33, 34). These seizures are readily apparent at 9 days postpartum and continue until death at approximately 3 weeks of age. In extensive complementation analysis, the coat color, opisthotonic, and lethality phenotypes are genetically inseparable (30). This observation implies that all three phenotypes are the consequence of mutation of a single gene, indicating that the dilute locus product(s) is critical for melanocyte morphology, neurological development, and juvenile survival.

Another class of dilute alleles was identified in the offspring of radiation-treated stocks (24, 30). Although these mutations were selected for their effect on the dilute locus, extensive complementation analysis indicated that the lesion associated with many of these mutations not only affected *d* but also extended into other loci that flank dilute. From this analysis, a complementation map of an approximately 5-centiMorgan (cM) region of mouse chromosome 9 could be derived (Fig. 1A) (24, 30). This region contains loci critical for melanocyte morphology (*d*), neurological development (*d* and Snell's waltzer [*sv*]), skeletal morphology (short ear [*se*]), and embryonic or juvenile survival (prenatal lethal 1 to 6 [*pl-1* to *pl-6*] and neonatal lethal 1 and 2 [*nl-1* and *nl-2*]). The genetic analysis predicted (30, 31) and the initial molecular analysis proved (24) that many of the radiation-induced mutations were caused by physical deletions which, in many cases, removed large segments of the chromosome. Therefore, this class of dilute alleles provides a resource not only for studying the *d* locus but also for accessing the other genetically defined loci that map in the dilute region of mouse chromosome 9.

Molecular access to the dilute region was afforded by the elucidation of the physical basis of the original dilute coat

* Corresponding author.
† Present address: Institute for Arthritis and Autoimmunity, West Haven, CT 06516.

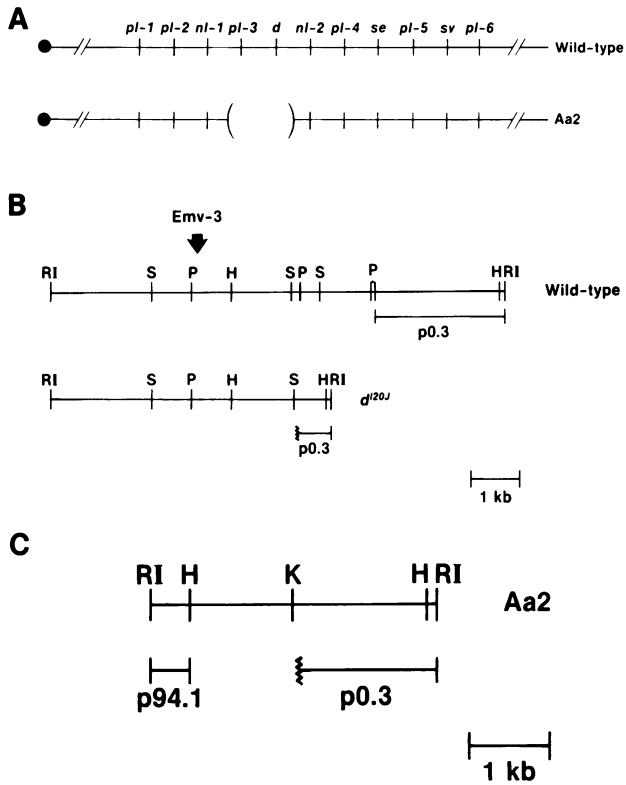

FIG. 1. Genetic map of the dilute-short ear region of mouse chromosome 9 and restriction maps of deletion breakpoint fusion fragments associated with d^{l20J} and Aa2 alleles. (A) Genetic map of chromosome 9 in wild-type and Aa2 dilute prenatal-lethal alleles. The map represents an approximately 5-cM region of this chromosome; no correlation with physical distance is implied. The order of the functional groups is based on the complementation analysis of the radiation-induced dilute alleles (24, 30). Parentheses indicate the chromosomal region deficient in the Aa2 dilute prenatal lethal allele. Symbol: ●, centromere. Abbreviations: *d*, dilute; *se*, short ear; *sv*, Snell's waltzer; *pl-1* to *pl-6*, prenatal lethal 1 to 6; *nl-1* and *nl-2*, neonatal lethal 1 and 2. (B) Restriction map of dilute-lethal^{20J} deletion breakpoint fusion fragment and the corresponding wild-type fragment. Lines below each map indicate the location of sequences homologous to the unique-sequence genomic probe p0.3 within the 9.2-kb wild-type (6) and 5.5-kb d^{l20J} (22) *Eco*RI restriction fragments. The solid arrow indicates the position of the *Emv-3* proviral integration site in the dilute-viral (d^v) allele. Abbreviations: RI, *Eco*RI; S, *Sst*I; P, *Pst*I; H, *Hin*dIII. (C) Restriction map of the dilute prenatal lethal Aa2 deletion breakpoint fusion fragment. Lines below the map indicate the location of sequences homologous to the p0.3 and p94.1 unique-sequence genomic probes within the 3.3-kb *Eco*RI restriction fragment (24). Abbreviations: RI, *Eco*RI; H, *Hin*dIII; K, *Kpn*I.

color mutation. Genetic and molecular studies showed that this spontaneous dilute mutation of the mouse fancy was causally associated with an ecotropic murine leukemia provirus, *Emv-3* (14). Because of this association, the original *d* coat color mutation is now termed dilute-viral (d^v). The presence of the provirus provided the molecular entry point for the isolation of the dilute gene (6). One unique-sequence probe (p0.3; Fig. 1B) that flanks the *Emv-3* integration site has been invaluable for examining the genomic organization of spontaneous and radiation-induced dilute alleles (21, 24), identifying dilute gene transcripts, and isolating dilute cDNA clones (P. K. Seperack, M. C. Strobel, N. G. Copeland, and N. A. Jenkins, manuscript in preparation).

By using the p0.3 genomic probe, restriction fragment length polymorphisms were detected in two dilute alleles: one spontaneous dilute-lethal allele, d^{l20J} (21), and one radiation-induced dilute prenatal lethal allele, Aa2 (24). Restriction mapping of these two restriction fragment length polymorphisms showed that these mutations were clearly associated with deletions. In this study, DNA sequence analysis of the deletion breakpoint fusion fragments associated with the d^{l20J} and Aa2 mutations has been accomplished, allowing precise definition of the deletion termini and the junction between these termini. This represents the first DNA sequence analysis of a radiation-induced, germ line mutation in the mouse. Comparison of the wild-type genomic sequence with those of the dilute cDNAs and the d^{l20J} deletion breakpoint fragment has defined the molecular consequences of the d^{l20J} mutation. Finally, sequence analysis of the Aa2 deletion breakpoint fusion fragment and the corresponding wild-type sequences has facilitated a chromosome jump that has provided molecular access to a gene proximal to *d* on mouse chromosome 9.

MATERIALS AND METHODS

Mouse strains. C57BL/6J, C57BL/6J-$d^v se/d^v se$ and C57BL/6J-$d^{l20J}/d^v se$ mice used in this study are maintained in this laboratory. Mice carrying radiation-induced mutations were produced at the Biology Division, The Oak Ridge National Laboratory, Oak Ridge, Tenn., and are maintained as previously described (24, 30).

Genomic and cDNA clones. The genomic cloning and restriction maps of the 5.5-kilobase-pair (kb) *Eco*RI d^{l20J} deletion breakpoint fusion fragment, the corresponding 9.2-kb *Eco*RI wild-type fragment (Fig. 1B), the 3.3-kb *Eco*RI Aa2 deletion breakpoint fusion fragment (Fig. 1C), and the 2.3-kb *Eco*RI wild-type fragment that corresponds to the 5′ end of the Aa2 deletion (see Fig. 4) have been described previously (6, 21, 24). The dilute cDNA clones were isolated from a λgt10 library constructed from B16 mouse melanoma cell line RNA (21; Seperack et al., in preparation). The B16 mouse melanoma cell line is wild type at dilute.

DNA sequence analysis. All genomic, cDNA, and derived subclones were cloned into M13mp18 and/or M13mp19 bacteriophage (39) or Bluescript (Stratagene Inc.) vectors for DNA sequencing. M13 phage DNA subclones were sequenced by using the 17-base-pair (bp) universal sequencing primer and sequence-specific oligonucleotide primers (17 to 23 bp) essentially by the method of Sanger et al. (32). The d^{l20J} deletion breakpoint (954-bp) and the corresponding wild-type (4,534-bp) regions were sequenced from subclones derived from the 5.5- and 9.2-kb *Eco*RI genomic clones, respectively. The 3.3-kb (3,356-bp) Aa2 deletion breakpoint fusion fragment and the 2.3-kb (2,231-bp) wild-type fragment corresponding to the 5′ end of the Aa2 deletion breakpoint fusion fragment were sequenced in their entirety. Each subclone was sequenced in both directions or at least twice in one direction. Sequencing of cDNA clones will be described separately (Seperack et al., in preparation).

Sequencing reagents were obtained from Pharmacia, Inc. (^{32}P Nucleotide Reagent Kit); Bethesda Research Laboratories, Inc. (Klenow fragment of DNA polymerase I); and United States Biochemical Corp. (Sequenase). [α-^{32}P]ATP and [α-^{35}S]ATP were obtained from Amersham Corp. Sequencing reactions were resolved on 6% acrylamide-bisacrylamide (19:1) Tris-borate-EDTA gels that contained 8 M urea. Sequence data were compiled and analyzed by using the DNA sequence programs of Stephens for the IBM PC

computer (36). Additional analysis of DNA sequences (10) was done with the assistance of Gary Smythers, Advanced Scientific Computing Laboratory, Program Resources Inc., National Cancer Institute-Frederick Cancer Research Facility, Frederick, Md.

Southern and Northern (RNA) blot analyses. High-molecular-weight DNA was extracted from tissues or cell lines as previously described (15). Yeast DNA was the gift of David Garfinkel; *Drosophila* DNA was the gift of Dennis McKearin. Restriction endonuclease digestions and Southern blot analyses were carried out essentially as described by Siracusa et al. (35). However, the "Zoo" blot was hybridized and washed under conditions of low stringency: blots were hybridized at 55°C under standard salt conditions (35) and were washed at 55 to 60°C in 1× SSCP–0.1% sodium dodecyl sulfate (15). Mouse brain RNA was prepared and analyzed as described previously (21).

RESULTS

DNA sequence analysis of the dilute-lethal (d^{l20J}) and dilute prenatal lethal (Aa2) deletion breakpoint fusion fragments. The dilute allele d^{l20J} arose spontaneously in the (C57BL/6J × DBA/2J)F_1 breeding colony of The Jackson Laboratory, Bar Harbor, Maine, and was kindly provided by Hope Sweet. The mutation arose on the C57BL/6J chromosome and was recognized by noncomplementation of the dilute-viral allele (d^v) carried on the DBA/2J chromosome (21). In addition to the dilute coat color, d^{l20J} homozygotes manifest opisthotonic convulsions until their death at approximately 3 weeks postpartum, clearly defining d^{l20J} as a dilute-lethal allele (30, 33, 34).

Using a dilute locus unique-sequence genomic probe (p0.3 [Fig. 1B]), analysis indicated that a unique restriction fragment cosegregated with the d^{l20J} mutation (21). p0.3 recognizes a 9.2-kb *Eco*RI fragment in wild-type DNA (6), but an approximately 5.5-kb fragment in d^{l20J} DNA (21) (Fig. 1B). Comparative restriction mapping of the two *Eco*RI fragments suggested that the unique d^{l20J} restriction fragment represents a deletion breakpoint fusion fragment resulting from an interstitial deletion of the wild-type fragment (Fig. 1B) (21). The 5′ end of the deletion lies approximately 2 kb 3′ of the d^v proviral integration site, while the 3′ end of the deletion lies within p0.3 sequences (Fig. 1B).

DNA sequence analysis of the deletion breakpoint fusion fragment confirmed that the d^{l20J} allele is caused by a discrete deletion of 3,580 bp. Nearly 2 kb of p0.3 sequence is deleted; 624 bp of p0.3 is retained in the breakpoint fusion fragment. No extraneous nucleotides are present at the deletion breakpoint; rather, the mutant DNA sequence is strictly colinear with the homologous wild-type sequences 5′ and 3′ of the deletion termini, respectively (Fig. 2A).

Examination of the sequences near the d^{l20J} deletion breakpoint (Fig. 2A, nucleotide 129) indicates no significant homologies between the respective wild-type sequences 5′ and 3′ of the deletion breakpoint or the deleted sequences immediately adjacent to the breakpoint. Furthermore, the sequences closely flanking the breakpoint junction represent exon sequences of the dilute gene (Fig. 2A). No homologies to repeated genomic elements are observed. The only notable sequence features at the deletion breakpoint are the A+T-rich nature of the junction region and the presence of a pair of inverted repeats (AACAGGT and ACCTGTT, beginning at nucleotides 118 and 165, respectively) that flank the deletion breakpoint. Computer-derived structural analysis shows that these inverted repeats could assume a secondary structure that would bring the deletion termini into proximity and could stabilize the free DNA ends, facilitating ligation to create the deletion breakpoint fusion fragment.

The Aa2 dilute prenatal lethal allele, also designated 19R145H (24), arose in the offspring of a stock in which spermatogonia were irradiated with a single dose of neutrons (145 rads; L. B. Russell and E. M. Rinchik, personal communication). Complementation analysis indicated that the Aa2 allele is a multilocus deficiency, affecting the dilute locus and prenatal lethal-3 (*pl-3*; Fig. 1A) functional unit (24, 30).

By using the p0.3 genomic probe, a unique restriction fragment was associated with this mutation (24). Restriction enzyme mapping showed that this unique fragment represents a deletion breakpoint fusion fragment (Fig. 1C) (24). Consistent with the genetic analysis, the 3′ end of the Aa2 deletion lies within the dilute locus, specifically within p0.3 sequences; 1,624 bp of p0.3 is retained in the breakpoint fusion fragment. At the proximal (5′) end of the breakpoint fragment, a 510-bp unique-sequence probe, p94.1, was identified (24). The precise genomic distance separating p94.1 and p0.3 is unclear at present. Pulse-field and contour-clamp gel electrophoresis analysis is in progress to define the physical distance between these two probes. The genetic analysis, which shows that the Aa2 deficiency affects both *d* and *pl-3*, suggests that the physical distance must be large enough to encompass all or part of these two loci.

Sequence analysis of the Aa2 deletion breakpoint fusion fragment indicates few notable features at the deletion junction. The junction is defined by the dinucleotide CT (Fig. 2B, nucleotides 131 and 132), which is present at each deletion terminus in the wild-type sequence. The sequences 5′ and 3′ of the junction are colinear with the corresponding wild-type sequences, and no extra nucleotides appear at the junction. Computer-derived structural analysis of the junction sequences indicates no additional homologies that could have stabilized the rejoining of the free broken ends to form the deletion breakpoint fusion fragment.

Molecular consequences of the dilute-lethal (d^{l20J}) deletion. Previous studies have shown that the molecular basis of the original dilute coat color mutation, now termed dilute-viral (d^v), is the integration of the murine ecotropic provirus, *Emv-3*, into a noncoding region at or near the dilute locus (6, 13). Although these studies provided the genomic probes for analysis of the region flanking the proviral integration site, they did not precisely define a genomic region critical for dilute gene function. Molecular elucidation of the dilute-lethal allele d^{l20J} provides such a definition. The correlation between a discrete deletion and this dilute-lethal allele implies that the deleted sequences, possibly those present in p0.3, must be critical for dilute gene function or expression. By using the p0.3 probe, Northern (RNA) blot analysis detected dilute gene transcripts in RNA derived from the B16 mouse melanoma cell line. Subsequently, p0.3 was used to isolate clones from a B16 cDNA library (Seperack et al., in preparation).

Comparison of the DNA sequence of the cDNA clones and the wild-type genomic sequence in the region flanking the proviral integration site has elucidated the genomic organization in this discrete region of the dilute locus. The *Emv-3* proviral integration site lies within an intron (Fig. 3), consistent with the observation that the provirus is located in a noncoding region (6, 13). At present, five dilute gene exons have been identified in the discrete region flanking the proviral integration site. Analysis of six independent dilute cDNA clones indicates that these five exons can be differ-

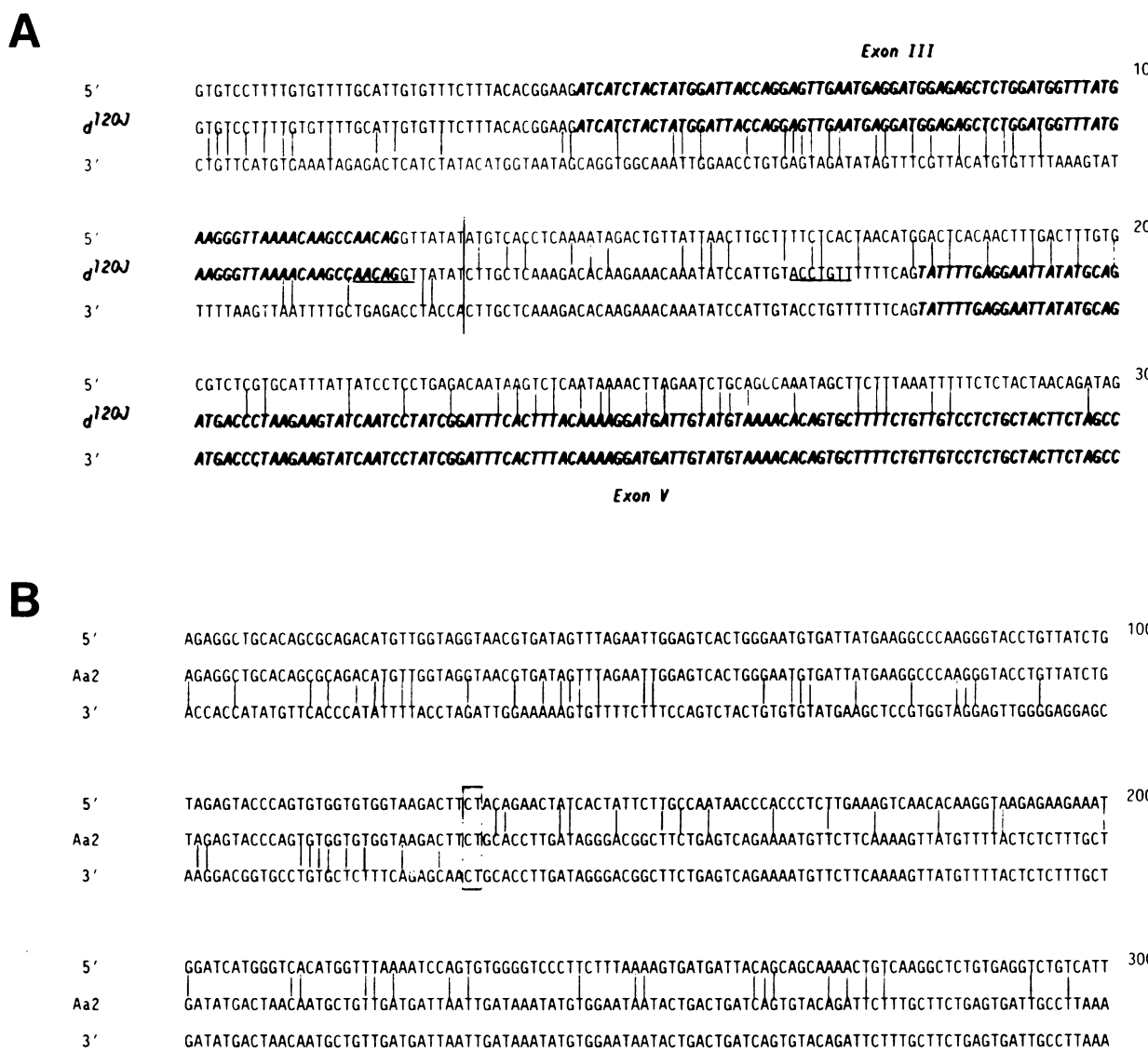

FIG. 2. Sequences of regions flanking the deletion breakpoint in the d^{l20J} and Aa2 alleles. (A) Sequences of the wild-type and d^{l20J} deletion breakpoint. The breakpoint is indicated by the vertical line. The middle sequence is the d^{l20J} deletion breakpoint fusion fragment; upper and lower sequences are the respective wild-type sequences at the 5' and 3' ends of the deletion. Homologies between the d^{l20J} and noncolinear sequence are indicated by the short vertical lines. Underlined sequences highlight the inverted repeats that flank the deletion breakpoint. Boldface letters indicate exon sequences of the dilute gene. (B) Sequences of the wild-type and Aa2 deletion breakpoint. The breakpoint is indicated by a box. The middle sequence is the Aa2 deletion breakpoint fusion fragment; upper and lower sequences are the respective wild-type sequences at the 5' and 3' ends of the deletion. Homologies between Aa2 and noncolinear sequences are indicated by the short vertical lines.

entially spliced to produce three distinct transcription patterns for this region (Seperack et al., in preparation). However, each splicing pattern incorporates exon IV; exon IV is totally removed by the d^{l20J} deletion (Fig. 3).

Molecular analysis of the dilute prenatal lethal Aa2 deletion breakpoint fusion fragment affords access to a previously undefined gene. The molecular analysis of deletion breakpoint fusion fragments associated with the radiation-induced dilute alleles will provide access to genomic sequences that lie at a distance from the dilute gene, potentially affording direct physical entry to other loci that map in the dilute region. Analysis of the DNA sequence of the Aa2 deletion breakpoint fusion fragment and the wild-type counterparts has confirmed this expectation.

Translation of the DNA sequence of the region flanking and including p94.1 indicated the presence of an open reading frame (ORF) of at least 460 nucleotides (Fig. 4A). By using a probe that encompasses part of the ORF (Fig. 4A, *Sal*I-*Hin*dIII fragment), Northern blot analysis indicated that two transcripts of 10.5 and 5.0 kb are present in C57BL/6J brain poly(A)$^+$ RNA (Fig. 4B). Additional analysis has shown that these transcripts are present in RNA derived from every mouse tissue and cell line examined; rich sources of these transcripts are adult testes and both embryonic and adult brain (Fig. 4B; data not shown). Recently, cDNA clones that include this ORF have been isolated from a C57BL/6J adult brain cDNA library (kindly provided by Elizabeth Lacy, Sloan Kettering Institute, New York, N.Y.).

In addition to being expressed in every tissue and cell line

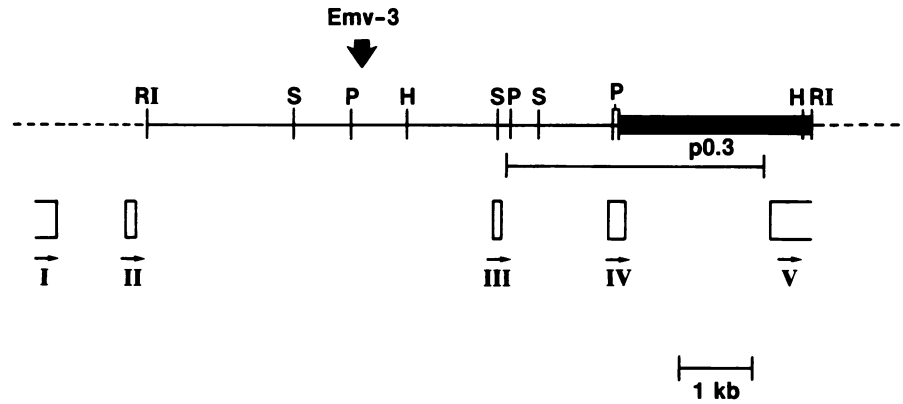

FIG. 3. Intron-exon organization of the dilute gene in the genomic region affected by the d^{l20J} deletion. The horizontal line below the map indicates the genomic region removed by the d^{l20J} deletion. ■, Region included in the p0.3 genomic probe. Boxes I to V indicate the exons present in dilute cDNAs; arrows below the boxes indicate the direction of transcription of the dilute gene. The genomic dilute locus extends both 5′ and 3′ of the discrete genomic region depicted. The dotted line on the restriction map indicates the positions of exons within this genomic region that have not been precisely mapped. The heavy arrow indicates the position of the *Emv-3* proviral integration site in the dilute-viral (d^v) allele. Abbreviations: RI, *Eco*RI; S, *Sst*I; P, *Pst*I; H, *Hin*dIII.

examined, this ORF appears to be highly conserved in evolution. The *Sal*I-*Hin*dIII probe recognizes the expected *Eco*RI fragments, of 2.0 and 2.3 kb, in C57BL/6J mouse spleen DNA (Fig. 4C, lane o). Furthermore, strongly homologous, apparently single-copy sequences are present in the DNA from all warm-blooded animals examined. Chicken, turkey, hamster, guinea pig, rat, rabbit, dog, cat, mink, sheep, and human DNAs exhibit strong homologies upon hybridization with this probe (Fig. 4C, lanes d to n). Weaker homologies are observed with *Xenopus* DNA and, possibly, *Drosophila* and yeast DNAs (Fig. 4C, lanes a to c).

The cumulative evidence of an ORF that is widely expressed and evolutionarily conserved implies that this ORF represents the coding sequence of a gene, designated the p94.1 gene. The ORF does not share sequence homology with the extant dilute cDNAs, and the nature and tissue specificity of the p94.1 gene transcripts are distinctly different from those of the dilute transcripts. The p94.1 gene transcription pattern is unaltered in brain RNA derived from d^v and d^{l20J}, alleles in which the dilute transcripts are quantitatively or qualitatively altered (Fig. 4B) (21; Seperack et al., in preparation). Therefore, these new transcripts are not dilute locus products but, rather, the products of a previously undefined gene proximal to the dilute locus.

From the genetic and molecular data, a prediction of the identity of the p94.1 gene can be made. Three radiation-induced mutations, Aa1, Aa2, and Aa3, affect only the dilute locus and the proximal prenatal lethal-3 (*pl-3*) functional unit (30). The initial molecular analysis predicted that the Aa1 allele would contain the smallest deficiency affecting the chromosomal interval from *pl-3* to *d*, while the Aa3 deletion would extend proximally beyond the endpoint of the Aa2 deletion (Fig. 5A) (24). Using a p94.1 gene cDNA probe, we performed Southern blot analysis of wild-type, Aa1, Aa2, and Aa3 DNAs (Fig. 5B). The approximately 3-kb cDNA probe recognizes 28 to 30 kb of genomic *Eco*RI fragments in DBA/2J and C57BL/6J DNAs (Fig. 5B); these genomic fragments encompass and extend 3′ from the p94.1 ORF. Since homozygotes for the Aa1, Aa2, or Aa3 chromosome die in utero, DNA was obtained from heterozygotes in which the mutant chromosome is balanced with a chromosome that exhibits either a DBA/2J (Aa1 and Aa2) or C57BL/6J (Aa3) restriction pattern. In addition to fragments ascribable to the balancer chromosome, two unique *Eco*RI fragments are observed: the expected 3.3-kb deletion breakpoint fusion fragment in Aa2 DNA (24) and an approximately 9.2-kb fragment in Aa1 DNA. The unique Aa1 fragment is a candidate for a deletion breakpoint fusion fragment. No polymorphic fragments are detected in Aa3 DNA; rather, the reduced intensity of all bands recognized in Aa3 DNA is consistent with the total deletion of this region in the Aa3 chromosome. Therefore, each allele that, by complementation analysis, includes the *pl-3* functional unit exhibits DNA alterations within an approximately 30-kb genomic region encoding part of the p94.1 gene.

DISCUSSION

The rich collection of *d* alleles is providing a rare opportunity to analyze a complex mammalian locus at a level usually possible only in lower eucaryotes and procaryotes. As illustrated in this study, elucidation of the physical lesions associated with two dilute alleles, dilute-lethal^{20J} (d^{l20J}) and dilute prenatal lethal Aa2, has precisely defined an essential region of the dilute gene and has identified a gene in the chromosomal region flanking dilute. The ongoing generation of genomic and cDNA probes for the dilute gene (and other genes in the dilute region) will provide the resources to examine additional spontaneous and mutagen-induced alleles, allowing a precise elucidation of the critical residues and regions of these genes. Furthermore, molecular analysis of these germ line mutations will provide a unique opportunity to examine, in a well-defined mammalian system, the products of the events that lead to both spontaneous and induced mutations.

DNA sequence analysis of the spontaneous d^{l20J} and the radiation-induced Aa2 deletion breakpoint fusion fragments indicates that these junction fragments must have been created by nonhomologous recombination events. No extensive sequence homologies are observed at the junction of the deletion termini (Fig. 2). Furthermore, these termini were precisely rejoined to create a flush junction (26). No extraneous nucleotides of unknown origin are included at the junction. This observation is in marked contrast to the insertion junctions that have been found in association with other nonhomologous breakage-reunion events, such as the incorporation of DNA into the genome of transfected cells, chromosome translocations and immune system rearrange-

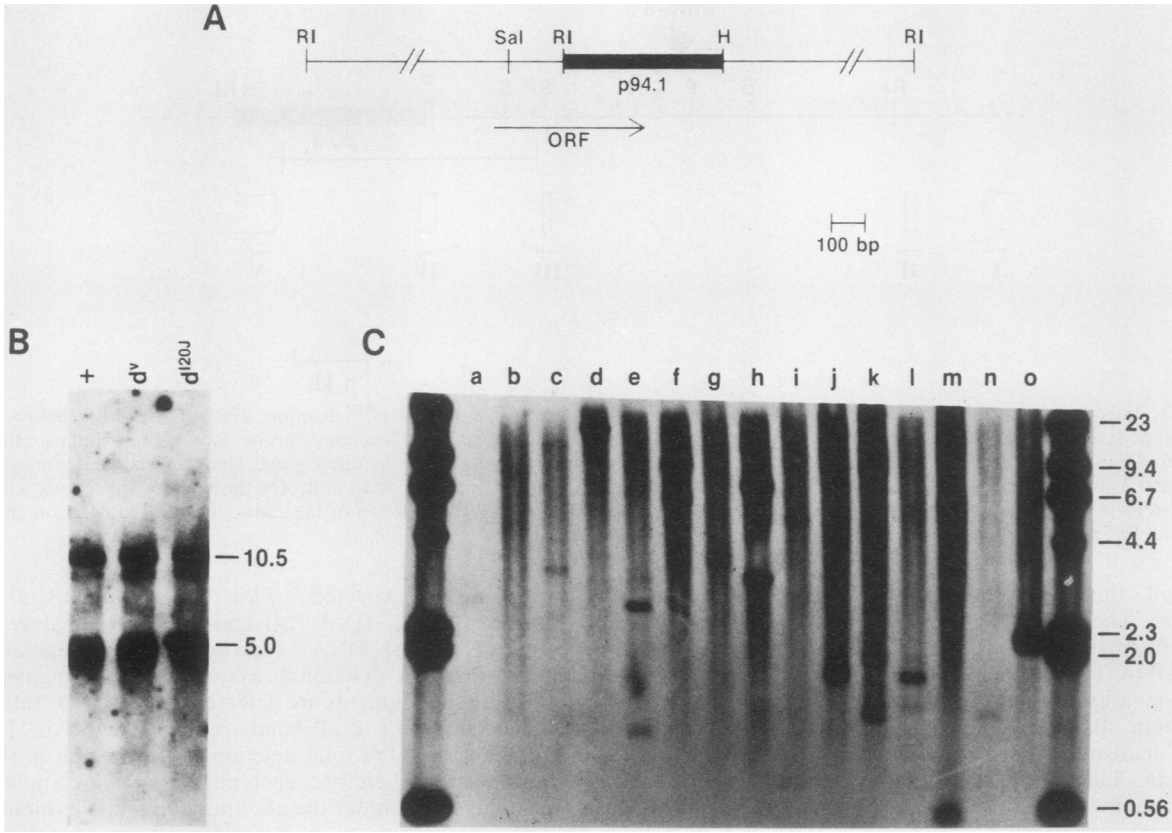

FIG. 4. Genomic position, expression, and evolutionary conservation of the ORF associated with p94.1. (A) Restriction map of the genomic region encoding the p94.1-associated ORF. The arrow indicates the location and extent of the 460-bp ORF. ▬, Location of the p94.1 genomic probe. Abbreviations: RI, *Eco*RI; Sal, *Sal*I; H, *Hin*dIII. (B) Northern blot analysis of brain RNA from wild-type and dilute mutants. Poly(A)$^+$ brain RNA (5 μg) was resolved on 1% formaldehyde-agarose gels. RNA was transferred and hybridized as previously described (22). RNA was probed with the *Sal*I-*Hin*dIII restriction fragment that encompasses the p94.1-associated ORF (panel A). The size of detected transcripts was determined by comparison with RNA size markers resolved in a parallel lane. Lanes: +, wild-type RNA; d^v, dilute-viral RNA; d^{l20J}, dilute-lethal^{20J} RNA. (C) Evolutionary conservation of the p94.1-associated ORF. A 10-μg sample of each DNA, with the exception of lane n, in which 2 μg of DNA was used, was resolved on 0.9% agarose gels. DNA was transferred and hybridized as described in Materials and Methods. The Southern Zoo blot was probed with the *Sal*I-*Hin*dIII probe (see panel A). Molecular weight markers are a *Hin*dIII restriction endonuclease digest of λ DNA. Lanes: a, yeast DNA; b, *Drosophila* DNA; c, *Xenopus* DNA; d, chicken DNA; e, turkey DNA; f, hamster DNA; g, guinea pig DNA; h, rat DNA; i, rabbit DNA; j, dog DNA; k, cat DNA; l, mink DNA; m, sheep DNA; n, human DNA; o, C57BL/6J mouse DNA.

ments (26, 27), and deletions in the human β-globin gene (16, 19).

Spontaneous mutations must arise through normal cellular DNA replication or recombination events. The cellular events by which the d^{l20J} deletion was generated are unclear, although the nature of the deletion junction is not unique, bearing similarity to deletion mutations in the human retinoblastoma gene (4, 17), β-globin cluster (37), and the *Caenorhabditis elegans* myosin heavy-chain gene (*unc-54*) (23). The size of the d^{l20J} deletion (3,580 nucleotides) and the absence of terminal sequence homology are inconsistent with a direct error by DNA polymerase generating this deletion, as has been described for both procaryotic and eucaryotic deletions (1, 9, 22). Furthermore, the unique sequence of the DNA flanking the deletion termini appears to rule out an uneven crossing over between repetitive genomic elements, as suggested for spontaneous deletions in human β-globin, low-density lipoprotein receptor, adenosine deaminase, and growth hormone genes (3, 5, 28, 38).

As speculated for other spontaneous deletions (4, 8, 37), the d^{l20J} deletion could have occurred as a consequence of higher-order chromatin structure (reviewed in reference 11). The interaction between adjacent chromatin loops via the proteins that form the chromosome scaffold or nuclear matrix could closely associate distantly separated sequences, whereas the proteins of the nuclear matrix could serve to catalyze the breakage-reunion events to create the deletion. The DNA sequences associated with the nuclear scaffold-associated regions and some scaffold proteins (notably, DNA topoisomerase II) have been identified in *Drosophila melanogaster* (7, 11). In general, scaffold-associated regions have been found between genes, usually associated with transcriptional promoter elements (11). The d^{l20J} deletion clearly lies within the dilute gene, and the deleted region is smaller than that observed between adjacent scaffold-associated regions (4.5 to 112 kb) (7, 11). However, the A+T-rich nature of the deletion junction is similar to the sequences recognized by DNA topoisomerases, although neither a distinct DNA topoisomerase II (7) nor a topoisomerase I (2) consensus sequence is observed. However, such enzyme activities could be involved in the introduction of chromosome breaks, such as those that led to the d^{l20J}

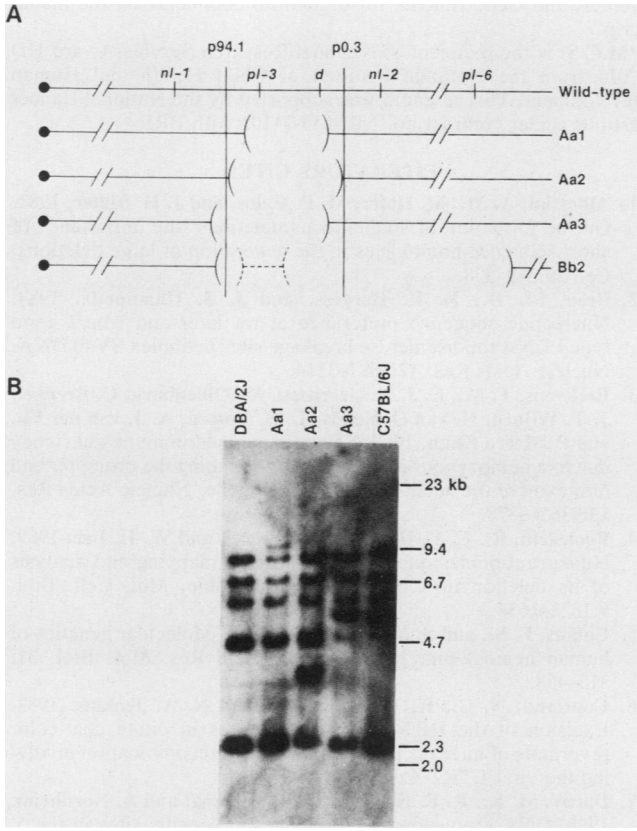

FIG. 5. Analysis of radiation-induced dilute prenatal lethal alleles that affect the prenatal-lethal 3 (*pl-3*) functional unit. (A) Genetic map of the region flanking dilute on mouse chromosome 9 in wild-type and mutant chromosomes. The map represents a discrete region flanking the dilute locus; no correlation with physical distance is implied. Parentheses indicate the chromosomal regions deficient in Aa1, Aa2, Aa3, and Bb2 radiation-induced mutant chromosomes; the dashed line indicates the region predicted, by the genetic analysis, to be present in the Bb2 chromosome (see Discussion). Locations of sequences homologous to the p0.3 and p94.1 genomic probes are indicated by the vertical lines. The solid circle represents the centromere. *d*, dilute; *nl-1* and *nl-2*, neonatal lethal 1 and 2; *pl-3* and *pl-6*, prenatal lethal 3 and 6. (B) Southern blot analysis of C57BL/6J, DBA/2J, Aa1, Aa2, and Aa3 DNAs with a p94.1 gene cDNA probe. DNA was prepared from adult animals heterozygous for the Aa1, Aa2, or Aa3 mutant chromosome. In these animals, the Aa1 and Aa2 chromosomes are balanced with a DBA/2J chromosome; the Aa3 chromosome is balanced with a C57BL/6J chromosome. An 8-μg sample of each DNA was cleaved with *Eco*RI and was resolved on 0.9% agarose gels. DNA was transferred and hybridized as described in Materials and Methods. The blot was probed with the 3.0-kb p94.1 gene cDNA described in Results. Molecular weight markers are a *Hin*dIII restriction endonuclease digest of λ DNA.

deletion. Another structural feature of the d^{l20J} deletion is the presence of inverted repeats flanking the junction. Inverted repeats, which can form a stable secondary structure that could align deletion termini, have been associated with spontaneous deletion junctions in somatic cells (22) and a deletion hot spot in *Escherichia coli* (1). Molecular analysis of other mammalian deletion mutations is necessary to clarify the sequences, structures and, potentially, enzymatic activities involved in the generation of spontaneous germ line deletions.

Ionizing radiation can cause chromosome or chromatid breaks. The radiation-induced Aa2 dilute prenatal-lethal allele arose in a stock in which males were irradiated with a single dose of neutrons. The mutation was detected in the progeny of matings occurring more than 7 weeks after irradiation. Therefore, the mutation must have occurred in a spermatogonium. This experimental protocol has been shown to be relatively effective in generating multilocus deletions, although less effective than neutron exposure to postgonial stages or oocytes (31). This difference in mutagenic efficiency may reflect the lesion-healing process or the selective retention of mutated chromosomes in different meiotic stages.

A multilocus deletion, such as the Aa2 deletion, must arise through the rejoining of ends generated by two separate chromosomal or chromatid breaks. Since the mutagenic events occurred in spermatogonia, these breaks could have occurred within a single homolog, followed by the loss of the intervening segment, or in separate chromosomes, followed by a nonreciprocal exchange event during meiosis. At this time, it is possible only to speculate on the factors that facilitate the rejoining event. Animal cells can efficiently undergo nonhomologous recombination events (26, 27). These events appear to be facilitated by short (1- to 5-nucleotide) regions of homology at the termini (22, 26, 27). Furthermore, deletions induced by irradiation of somatic cells have been correlated with sequence homologies or direct repeats in the region affected by the deletion (12, 18). The sequence analysis of the Aa2 deletion breakpoint fusion fragment is the first molecular characterization of a mouse germ line, radiation-induced mutation. Examination of additional germ line, radiation-induced deletion breakpoints will be necessary to determine whether brief sequence homologies, such as the CT dinucleotide, which defines the Aa2 deletion breakpoint, have any relevance to the ligation of broken chromosomal ends generated by ionizing radiation.

Elucidation of the molecular defect associated with the d^{l20J} allele has clearly defined a discrete genomic region that is critical for dilute gene function. The d^{l20J} deletion removes a single exon of the dilute gene (Fig. 3, exon IV). The dilute gene encodes at least three transcripts (21; Seperack et al., in preparation). However, each unique transcript includes exon IV, the exon that is deleted in the d^{l20J} allele. In each transcription pattern, this exon contains coding sequences of the dilute gene; therefore, deletion of exon IV directly removes information of the dilute gene. Furthermore, deletion of this 199-bp exon leads to a shift in the predicted translational reading frame of each mRNA. This frameshift results in the introduction of in-frame stop codons in exon V that would prematurely terminate two dilute transcripts and the substitution of the 3′ coding and noncoding sequences of the third transcript (Seperack et al., in preparation).

The deletion of a single exon in the d^{l20J} allele is sufficient to abrogate totally the production of wild-type levels and species of dilute mRNA (21), defining the d^{l20J} allele as a functional null mutation of the dilute locus. The association between a discrete, interstitial deletion of the dilute gene and the expression of the full range of dilute-associated phenotypes by d^{l20J} homozygotes strongly suggests that the coat color, neurological, and lethality phenotypes are caused by the mutation of a single gene, the dilute gene.

DNA sequence analysis of the deletion breakpoint fusion fragment associated with the radiation-induced Aa2 mutation has identified an ORF at the proximal end of the fragment. Subsequent Northern blot and Southern Zoo blot analyses have shown that this ORF is widely expressed and is highly conserved in evolution. By virtue of its physical

location and transcription pattern, the p94.1 gene is clearly a distinct gene proximal to dilute.

In the complementation analysis of the radiation-induced mutations, three alleles, Aa1, Aa2, and Aa3, were found to affect only the dilute and the proximal *pl-3* functional unit (30). Initial molecular analysis has predicted the physical relationship among these three deficiency mutations (Fig. 5A) (24). With a p94.1 gene cDNA clone, Southern blot analysis of these radiation-induced alleles has confirmed and extended these predictions. Within the approximately 30-kb genomic region recognized by this probe in wild-type DNA, a unique fragment is found associated with the Aa1 mutation (Fig. 5B). This observation implies that one end of the Aa1 deletion lies within 30 kb of the Aa2 deletion endpoint and within the genomic region encoding the p94.1 gene. Furthermore, as predicted, the genomic region recognized by this cDNA clone is totally deleted in the Aa3 chromosome (Fig. 5B). Therefore, the genetic and molecular analysis of these three radiation-induced alleles emphasizes the correlation between a genetic deficiency of the *pl-3* locus and the detection of genomic alterations in the region encoding the p94.1 gene, suggesting that the p94.1 gene represents the *pl-3* locus.

The present genetic and molecular data for additional radiation-induced alleles support the prediction that the p94.1 gene is the *pl-3* locus: alleles that are deficient for *pl-3* are also deleted for the p94.1 genomic probe (24) and, correspondingly, the p94.1 ORF. The single exception to this correlation is the radiation-induced Bb2 allele (Fig. 5A) (24). From the complementation analysis, the Bb2 chromosome was classified as deficient for dilute and the loci distal from dilute (*nl-2*, *pl-4*, *se*, *pl-5*, *sv*, and *pl-6* [Fig. 1A and 5A]), but not deficient for the proximal *pl-3* locus. However, the molecular analysis indicated that Bb2 DNA does not contain p94.1 sequences (24), implying that the p94.1 gene cannot represent the *pl-3* locus (Fig. 5A). Although the Bb2 chromosome complements most radiation-induced mutations that are deficient for the *pl-3* locus, the Bb2 allele does not complement the Aa1 mutation, the smallest deficiency that affects the *pl-3* locus. Clearly, the Bb2 chromosome presents an anomaly. Examination of Bb2 DNA with additional molecular probes may reveal a complex chromosomal rearrangement, such as two independent deletions or a deletion-inversion event, that may clarify the complicated molecular and genetic data on this mutation.

Preliminary experiments indicate that d^{Aa1}/d^{Aa1} homozygotes, which are deleted for part of *d* and *pl-3*, die between implantation and 12.5 days of gestation (T. Sarafi and E. M. Rinchik, personal communication). Experiments are in progress to examine the expression of the p94.1 gene in wild-type and d^{Aa1}/d^{Aa1} embryos to correlate the appearance of p94.1 gene transcripts with the time of death of *pl-3* homozygous embryos. Ultimately, proof of identity between the p94.1 gene and the *pl-3* functional unit will depend upon the isolation of mutations that affect only *pl-3* and, presumably, the product(s) of the p94.1 gene or the generation of transgenic mice in which the *pl-3* prenatal lethality is corrected by p94.1 gene cDNA constructs.

ACKNOWLEDGMENTS

We thank Liane Russell, Gene Rinchik, and Trina Sarafi, of the Biology Division, Oak Ridge National Laboratory, for providing the radiation-induced dilute alleles and for communicating unpublished data and Robin Handley and Linda Brubaker for preparation of the manuscript. We also thank Monica Justice, David Kingsley, John Mercer, and Gene Rinchik for thoughtful comments on the manuscript.

M.C.S. is the recipient of National Research Service Award HD 07014 from the National Institute of Child Health and Human Development. This research was supported by the National Cancer Institute under contract no. N01-CO-74101 with BRI.

LITERATURE CITED

1. **Albertini, A. M., M. Hofer, M. P. Calos, and J. H. Miller.** 1982. On the formation of spontaneous deletions: the importance of short sequence homologies in the generation of large deletions. Cell **29**:319–328.
2. **Been, M. D., R. R. Burgess, and J. J. Champoux.** 1984. Nucleotide sequence preference at rat liver and wheat germ type I DNA topoisomerase breakage sites in duplex SV40 DNA. Nucleic Acids Res. **12**:3097–3114.
3. **Berkvens, T. M., E. J. A. Gerritsen, M. Oldenburg, C. Breukel, J. T. Wijnen, H. van Ormondt, J. M. Vossen, A. J. van der Eb, and P. Meera Khan.** 1987. Severe combined immune deficiency due to a homozygous 3.2-kb deletion spanning the promoter and first exon of the adenosine deaminase gene. Nucleic Acids Res. **15**:9365–9378.
4. **Bookstein, R., E. Y.-H. P. Lee, A. Peccei, and W.-H. Lee.** 1989. Human retinoblastoma gene: long-range mapping and analysis of its deletion in a breast cancer cell line. Mol. Cell. Biol. **9**:1628–1634.
5. **Collins, F. S., and S. M. Weissman.** 1984. Molecular genetics of human hemoglobin. Prog. Nucleic Acid Res. Mol. Biol. **31**: 315–458.
6. **Copeland, N. G., K. W. Hutchison, and N. A. Jenkins.** 1983. Excision of the DBA ecotropic provirus in dilute coat-color revertants of mice occurs by homologous recombination involving the viral LTRs. Cell **33**:379–387.
7. **Darby, M. K., R. E. Herrera, H.-P. Vosberg, and A. Nordheim.** 1986. DNA topoisomerase II cleaves at specific sites in the 5′ flanking region of c-*fos* proto-oncogenes *in vitro*. EMBO J. **5**:2257–2265.
8. **Darras, B. T., and U. Francke.** 1987. A partial deletion of the muscular dystrophy gene transmitted twice by an unaffected male. Nature (London) **329**:556–558.
9. **de Jong, P. J., A. J. Grosovsky, and B. W. Glickman.** 1988. Spectrum of spontaneous mutation at the *APRT* locus of Chinese hamster ovary cells: an analysis at the DNA sequence level. Proc. Natl. Acad. Sci. USA **85**:3499–3503.
10. **Devereux, J., P. Haeberli, and O. Smithies.** 1984. A comprehensive set of sequence analysis programs for the VAX. Nucleic Acids Res. **12**:387–395.
11. **Gasser, S. M., and U. K. Laemmli.** 1987. A glimpse at chromosomal order. Trends Genet. **3**:16–22.
12. **Grosovsky, A. J., J. G. de Boer, P. J. de Jong, E. A. Drobetsky, and B. W. Glickman.** 1988. Base substitutions, frameshifts, and small deletions constitute ionizing radiation-induced point mutations in mammalian cells. Proc. Natl. Acad. Sci. USA **85**: 185–188.
13. **Hutchison, K. W., N. G. Copeland, and N. A. Jenkins.** 1984. Dilute-coat color-locus of mice: nucleotide sequence analysis of the d^{+2J} and d^{+Ha} revertant alleles. Mol. Cell. Biol. **4**:2899–2904.
14. **Jenkins, N. A., N. G. Copeland, B. A. Taylor, and B. K. Lee.** 1981. Dilute (*d*) coat-colour mutation of DBA/2J mice is associated with the site of integration of an ecotropic MuLV genome. Nature (London) **293**:370–374.
15. **Jenkins, N. A., N. G. Copeland, B. A. Taylor, and B. K. Lee.** 1982. Organization, distribution, and stability of endogenous ecotropic murine leukemia virus DNA sequences in chromosomes of *Mus musculus*. J. Virol. **43**:26–36.
16. **Jennings, M. W., R. W. Jones, W. G. Wood, and D. J. Weatherall.** 1985. Analysis of an inversion within the human beta globin gene cluster. Nucleic Acids Res. **13**:2897–2906.
17. **Lee, E. Y.-H. P., R. Bookstein, L.-J. Young, C.-J. Lin, M. G. Rosenfeld, and W.-H. Lee.** 1988. Molecular mechanism of retinoblastoma gene inactivation in retinoblastoma cell line Y79. Proc. Natl. Acad. Sci. USA **85**:6017–6021.

18. **LoMonaco, M. B., W. R. Lee, and S. H. Chang.** 1987. Identification of an X-ray induced deletion mutant flanked by direct repeats. Nucleic Acids Res. **15**:7641.
19. **Mager, D. L., P. S. Henthorn, and O. Smithies.** 1985. A Chinese $G_\gamma^+(A_{\gamma\delta\beta})^0$ thalassemia deletion: comparison to other deletions in human β-globin gene cluster and sequence analysis of the breakpoints. Nucleic Acids Res. **13**:6559–6575.
20. **Markert, C. L., and W. K. Silvers.** 1956. The effects of genotype and cell environment on melanoblast differentiation in the house mouse. Genetics **41**:429–450.
21. **Moore, K. J., P. K. Seperack, M. C. Strobel, D. A. Swing, N. G. Copeland, and N. A. Jenkins.** 1988. Dilute suppressor *dsu* acts semidominantly to suppress the coat-color phenotype of a deletion mutation, d^{l20J}, of the murine dilute locus. Proc. Natl. Acad. Sci. USA **85**:8131–8135.
22. **Nalbantoglu, J., D. Hartley, G. Phear, G. Tear, and M. Meuth.** 1986. Spontaneous deletion formation at the *APRT* locus of hamster cells: the presence of short sequence homologies and dyad symmetries at deletion termini. EMBO J. **5**:1199–1204.
23. **Pulak, R. A., and P. Anderson.** 1988. Structures of spontaneous deletions in *Caenorhabditis elegans*. Mol. Cell. Biol. **8**:3748–3754.
24. **Rinchik, E. M., L. B. Russell, N. G. Copeland, and N. A. Jenkins.** 1986. Molecular genetic analysis of the *dilute-short ear* (*D-SE*) region of the mouse. Genetics **112**:321–342.
25. **Rinchik, E. M., L. B. Russell, N. G. Copeland, and N. A. Jenkins.** 1985. The dilute-short ear (*d-se*) complex of the mouse: lessons from a fancy mutation. Trends Genet. **1**:170–176.
26. **Roth, D. B., T. N. Porter, and J. H. Wilson.** 1985. Mechanisms of nonhomologous recombination in mammalian cells. Mol. Cell. Biol. **5**:2599–2607.
27. **Roth, D. B., and J. H. Wilson.** 1986. Nonhomologous recombination in mammalian cells: role for short sequence homologies in the joining reaction. Mol. Cell. Biol. **6**:4295–4304.
28. **Russell, D. W., M. A. Lehrman, T. C. Sudhof, T. Yamamoto, C. G. Davis, H. H. Hobbs, M. S. Brown, and J. L. Goldstein.** 1986. The LDL receptor in familial hypercholesterolemia: use of human mutations to dissect a membrane protein. Cold Spring Harbor Symp. Quant. Biol. **51**:811–819.
29. **Russell, E. S.** 1948. A quantitative histological study of the pigment in the coat-color mutants of the house mouse. II. Estimates of the total volume of pigment. Genetics **33**:228–236.
30. **Russell, L. B.** 1971. Definition of functional units in a small chromosomal segment of the mouse and its use in interpreting the nature of radiation-induced mutations. Mutat. Res. **11**: 107–123.
31. **Russell, L. B.** 1986. Information from specific-locus mutants on the nature of induced and spontaneous mutations in the mouse, p. 437–447. *In* Genetic toxicology of environmental chemicals, part B. Genetic effects and applied mutagenesis. Alan R. Liss, Inc., New York.
32. **Sanger, F., S. Nicklen, and A. R. Coulson.** 1977. DNA sequencing with chain-terminating inhibitors. Proc. Natl. Acad. Sci. USA **74**:5463–5467.
33. **Searle, A. G.** 1952. A lethal allele of dilute in the house mouse. Heredity **6**:395–401.
34. **Silvers, W. K.** 1979. The coat-colors of mice, p. 83–90. Springer-Verlag, New York.
35. **Siracusa, L. D., L. B. Russell, N. A. Jenkins, and N. G. Copeland.** 1987. Allelic variation within the *Emv-15* locus defines genomic sequences closely linked to the *agouti* locus on mouse chromosome 2. Genetics **117**:85–92.
36. **Stephens, R. M.** 1985. A sequencer's sequence analysis package for the IBM PC. Gene Anal. Tech. **2**:67–75.
37. **Vanin, E. F., P. S. Henthorn, D. Kioussis, F. Grosveld, and O. Smithies.** 1983. Unexpected relationships between four large deletions in the human β-globin gene cluster. Cell **35**:701–709.
38. **Vnencak-Jones, C. L., J. A. Phillips III, E. Y. Chen, and P. H. Seeburg.** 1988. Molecular basis of human growth hormone gene deletions. Proc. Natl. Acad. Sci. USA **85**:5615–5619.
39. **Yanisch-Perron, C., J. Vieira, and J. Messing.** 1985. Improved M13 phage cloning vectors and host strains: nucleotide sequences of the M13mp18 and pUC19 vectors. Gene **33**:103–119.